

Spectroscopic detection of biological NO with a quantum cascade laser

L. Menzel^{1,*,**}, A.A. Kosterev¹, R.F. Curl¹, F.K. Tittel¹, C. Gmachl², F. Capasso², D.L. Sivco², J.N. Baillargeon², A.L. Hutchinson², A.Y. Cho², W. Urban³

¹Rice Quantum Institute, Rice University, Houston, TX 77251-1892, USA

²Bell Laboratories, Lucent Technologies, 600 Mountain Avenue, Murray Hill, NJ 07974, USA

³Institut für Angewandte Physik, Universität Bonn, Wegeler Str. 8, 53115 Bonn, Germany

Received: 1 November 2000/Revised version: 19 January 2001/Published online: 20 April 2001 – © Springer-Verlag 2001

Abstract. Two configurations of a continuous wave quantum cascade distributed feedback laser-based gas sensor for the detection of NO at a parts per billion (ppb) concentration level, typical of biomedical applications, have been investigated. The laser was operated at liquid nitrogen temperature near $\lambda = 5.2 \mu\text{m}$. In the first configuration, a 100 m optical path length multi-pass cell was employed to enhance the NO absorption. In the second configuration, a technique based on cavity-enhanced spectroscopy (CES) was utilized, with an effective path length of 670 m. Both sensors enabled simultaneous analysis of NO and CO₂ concentrations in exhaled air. The minimum detectable NO concentration was found to be 3 ppb with a multi-pass cell and 16 ppb when using CES. The two techniques are compared, and potential future developments are discussed.

PACS: 42.62.Be; 82.80.Ch; 87.64.Je

Sensitive, selective and on-line laser-based trace gas detection can be an effective tool in various aspects of non-invasive medical diagnostics. The detection and quantification of a number of gases such as NO, CO, CO₂ and NH₃ play an important role in monitoring biomedical functions [1–4]. In recent years, the detection of CO₂ in human breath has become a diagnostic technique (for example, for the detection of helicobacter pylori, which causes ventricular ulcers [5]). Detection of biomedically-produced NO and its chemical products is also important because of their critical role in human physiology. Nitric oxide (NO) is produced in the human body and controls different physiological (and pathophysiological) processes, such as the diameter of blood vessels and immune reactions, and it is present in neuronal tissue [6]. NO can be detected in exhaled human breath and is a marker for diseases like asthma or inflammatory processes [7, 8]. NO levels in breath range from several parts per billion by volume (ppb)

to several hundred ppb. To date, most medical laboratories rely on chemiluminescence-based devices such as the Sievers NOATM 280, which can measure NO concentration in air down to 1 ppb level with a time resolution of 0.2 s. However, the chemiluminescence approach suffers from several intrinsic limitations. The presence of other species in the gas sample can influence the results. For example, ammonia also produces a chemiluminescence signal [9], and water leads to quenching of the chemiluminescent reaction. Furthermore, the chemiluminescence technique is not isotopic selective.

An alternative approach to quantification of ultra-low concentrations of NO is the use of high-resolution infrared absorption spectroscopy (IAS). IAS has been demonstrated to be a sensitive and selective tool for the detection of different trace gas components in ambient air (see for example [10, 11]). NO has a strong fundamental absorption band near $\lambda = 5.2 \mu\text{m}$, which can be used for monitoring purposes [12, 13]. Specific absorption lines can be selected to avoid interference from other species such as CO₂ and H₂O absorbing in this spectral region. IAS is also intrinsically isotopically selective. Further sensitivity enhancement can be obtained with laser magnetic resonance spectroscopy (LMRS), which exploits the property of NO to rotate light polarization in a magnetic field [14, 15]. However, LMRS adds complexity, which may not be justified for medical instrumentation.

IAS requires a single-frequency light source with sufficient power. Recently developed cw and pulsed distributed feedback quantum cascade lasers (QC-DFB) can be utilized as a convenient spectroscopic mid-IR source [16] for implementation into IR absorption-based biomedical gas sensors. Presently, cw operation of QC-DFB lasers requires cryogenic cooling, which adds inevitable bulkiness to an optical cryostat. However, it is generally believed that near-room temperature cw QC-DFB lasers will be available in the future [17]. In this paper, we describe and compare two QC-DFB IAS-based approaches to detection of NO at ppb concentration levels that are typical for biological applications. In both cases, the same cw single-frequency QC-DFB laser, operating near $\lambda = 5.2 \mu\text{m}$, was used as a tunable mid-IR source.

*Corresponding author.

(Fax: +49-228/733-474, E-mail: menzel@iap.uni-bonn.de)

**Present address: Institut für Angewandte Physik, Universität Bonn, Wegeler Str. 8, Germany

1 NO concentration measurements in a multi-pass absorption cell

1.1 Experimental set-up of the sensor

In the first NO laser sensor architecture, an optical multi-pass cell (modified Herriott cell, New Focus model 5612) with an optical path length of 100 m was used to obtain a measurable absorption at low NO concentrations. A schematic of the experimental setup is shown in Fig. 1. The QC-DFB laser was mounted on a cold finger of an optical liquid nitrogen dewar. The strongly diverging cw QC-DFB laser output at $5.2\ \mu\text{m}$ was collected by a gold-coated 90° off-axis parabolic mirror with an effective focal length (EFL) of 76.2 mm and a diameter of 76.2 mm. The laser light was then collimated by a combination of another off-axis parabolic mirror (same diameter, EFL = 152.4 mm) and an uncoated BaF_2 lens ($f = 13\ \text{mm}$) into a quasi-parallel beam with a diameter of $\sim 4\ \text{mm}$. The laser radiation power measured after the BaF_2 lens reached 80 mW at the highest laser driving current of 900 mA. The laser beam was focused into the multi-pass cell with an $f = 500\ \text{mm}$ CaF_2 lens. The throughput of the multi-pass cell was measured to be 20%.

Most of our experiments were carried out at a sample gas pressure of 50 Torr in the cell. This pressure ensured sufficient spectral resolution for H_2O - CO_2 -NO mixtures without any noticeable decrease in absorption features. Working at reduced pressure is also practicable for medical applications because it decreases the volume of an atmospheric pressure gas sample required to fill the multi-pass cell.

As a consequence of having high QC laser power, it was possible to use a compact room temperature HgCdZnTe detector (Boston Electronics PDI-10.6, active area $1\ \text{mm}^2$, external dimensions $\varnothing = 13\ \text{mm}$, $l = 40\ \text{mm}$). A 200 MHz DC-coupled preamplifier and an additional amplifier (Stanford Research SR560) subsequently amplified the detector output, with bandpass cut-off frequencies set at 0.1 Hz to 30 kHz. Such bandpass filtering resulted in considerable suppression of detector noise without reducing the absorption signal. The data were subsequently acquired and

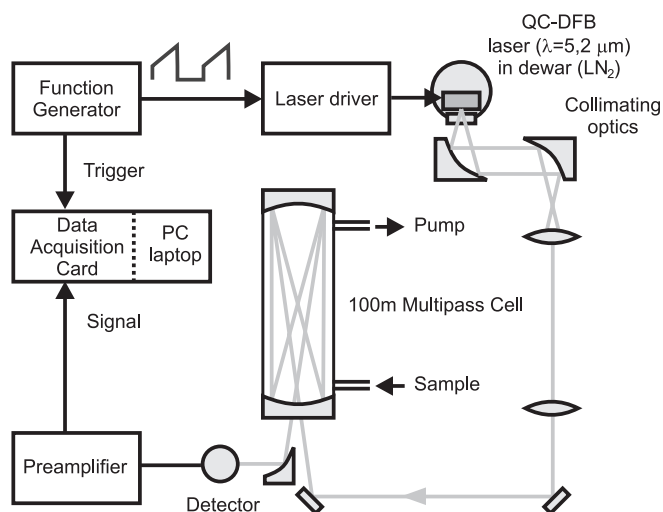


Fig. 1. Schematic of the QC-DFB laser-based spectrometer

processed with a data acquisition card (maximum sampling rate 2×10^5 samples/s, 16-bit resolution) and a laptop computer.

The QC laser frequency could be tuned using both temperature and current. The temperature tuning coefficient for this kind of laser is typically $0.08\text{--}0.09\ \text{cm}^{-1}/\text{K}$. In our experiments, laser temperature was not actively controlled but determined by the heat dissipation of the laser and the heat transfer through the cold finger. The laser current of 0 to 1 A was supplied by a low-noise current driver, which was controlled by an external waveform synthesizer. A typical $\sim 5\ \text{ms}$ -long current pulse waveform, as used in our experiments, is shown as the dotted line in Fig. 2. Such a pulse length made the laser operate in a quasi-cw mode. The duty cycle was set to 50% in order to select the appropriate laser frequency region and to minimize heating of the QC laser. A wave number range of $1918.3\ \text{cm}^{-1}$ to $1919.2\ \text{cm}^{-1}$ was scanned with a repetition rate of 100 Hz. Frequency calibration using the known frequencies of one H_2O and five CO_2 absorption lines in the breath spectrum yielded an almost linear relationship between current and frequency, with $dv/dI = -9.6\ \text{cm}^{-1}/\text{A}$. This calibration allowed the identification of the NO absorption.

Interference fringes from optical components and the multi-pass cell were the main factor limiting the detection sensitivity. To improve the signal-to-noise ratio (SNR), absorption signals were averaged over a number of scans (typically 200 to 10 000). A varying mechanical force was manually applied to the multi-pass cell mirror mounts during the data acquisition, which resulted in a reduction in optical fringes by a factor of 5. Additional suppression of interference fringes was obtained when the laser line-width was artificially broadened by applying a small amplitude sinusoidal laser current modulated at 24.7 kHz. The resulting laser line broadening was smaller than the width of pressure-broadened lines at 50 Torr. The remaining noise level was approximately 10^{-4} of the transmitted intensity.

Previous investigations showed that the SNR follows a \sqrt{n} dependence on the number of averaging n up to 100 scans, at which point the increase slows down. Averaging over 10 000 scans (which takes 200 s, due to software delays) gives a further 2.5 times improvement in the SNR compared to 100 scans.

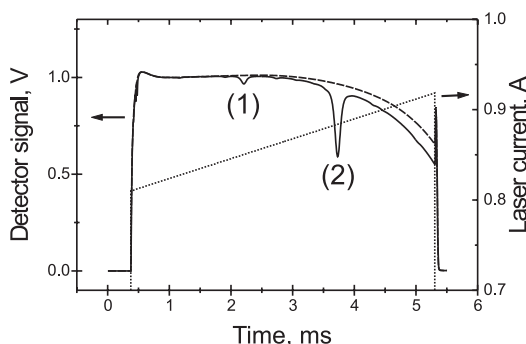


Fig. 2. Transmission of the multi-pass cell filled with pure nitrogen (dashed line) and a breath sample (solid line) at 50 Torr as a function of time. The temporal dependence of laser current is also depicted (dotted line). (1) H_2O , $1918.860\ \text{cm}^{-1}$; (2) CO_2 , $1918.585\ \text{cm}^{-1}$

1.2 Absorption signals in breath samples

Two examples of the transmitted intensity are depicted in Fig. 2. The dashed line shows the signal for a multi-pass cell filled with nitrogen at 50 Torr. The solid line corresponds to the transmission of exhaled air at 50 Torr. The difference between the two curves at times approaching 5 ms is due to the shoulders of strong H₂O absorption lines at 1918.035 cm⁻¹ and 1918.007 cm⁻¹. The air was exhaled via the nose and collected in a plastic bag prior to transfer into the cell. The NO was detected from the unresolved components of the R12.5 transition at 1918.702 and 1918.705 cm⁻¹.

To determine the absorption spectrum of a gas inside the cell, the absorption of the ambient air outside the cell must be subtracted. This was done using the transmission spectrum of the nitrogen-filled cell. In addition, the remaining base line distortion caused by the wing of the strong water absorption at ~ 1918 cm⁻¹ was removed in order to derive the NO absorption. Eight data points were selected in small near-zero second derivative regions between the absorption lines of carbon dioxide and water, and interpolated with a spline function to obtain this correction. The interpolating curve was then considered as a new baseline.

Figure 3 shows the spectra of two exhaled air samples with a corrected baseline. A healthy human subject exhaled one sample through the nose and another through the mouth. As described previously, in both measurements the exhaled air was collected in a plastic bag and afterwards filled the evacuated multi-pass cell at a pressure of 50 Torr. The H₂O and CO₂ absorption of both samples was almost the same, but the NO concentration obtained breathing via the nose was approximately 7.7 times higher than for exhalation through the mouth. The reason for this large difference is the fact that the NO production in the upper airways is much higher in comparison to the production in the alveolar region in the lower respiratory tract [14].

The NO concentration was evaluated to be 13 ppb in the mouth-exhaled sample and 100 ppb in the nose-exhaled sample. These numbers were obtained using a Voigt line shape fit and simulations made with the HITRAN'92 database. The residual of the best fit was interpolated with the same line shape at different positions on the wave number scale in order to determine the SNR. This procedure resulted in a SNR of 5

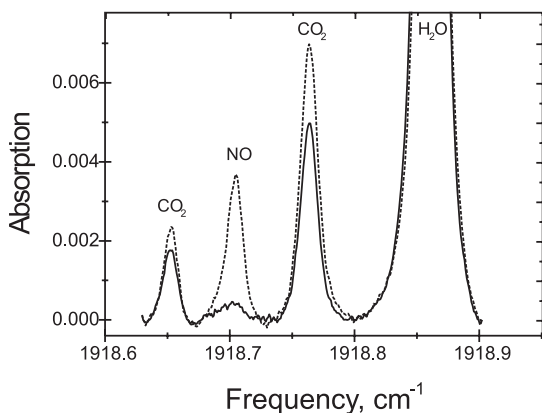


Fig. 3. Absorption spectrum of a breath sample from the nose (*dashed line*) and the mouth (*solid line*) at 50 Torr in the 100 m path length multi-pass cell

for the mouth-exhaled signal, which implies a minimum detectable NO concentration of 2.6 ppb. Hence this QC-DFB laser-based spectrometer is suitable for the detection of biological NO at ppb concentration levels.

2 NO concentration measurements using cavity-enhanced spectroscopy (CES)

2.1 The CES spectrometer

The second technique evaluated by us is based upon an effective enhancement of the path length in a ultrahigh-finesse optical cavity. This approach has recently become possible due to the technological progress in the fabrication of highly reflective, low loss dielectric mirrors in the IR spectral region. The implementation of this method is facilitated by the high power of the QC-DFB laser.

To detect the absorption, the throughput of the optical cavity is monitored in the same way as for a multi-pass cell. The alignment of the cavity and the laser is chosen such that the highest number of cavity transverse modes are excited. This creates a dense spectrum of cavity modes and enables us to consider such a light-cavity interaction as non-coherent, in particular when the mechanical instability of the cavity mirrors is considered. This technique, known as cavity-enhanced spectroscopy (CES), was first demonstrated by Engeln et al. [18] in the visible part of the spectrum. CES does not require time-resolved measurements, unlike cavity ring-down spectroscopy (CRDS), where the decay time of cavity modes is measured instead of the averaged transmitted intensity. CES was successfully used to detect ammonia by its overtone absorption in the near IR [19]. The transmission of the cavity in a purely non-coherent approximation in case of perfect spatial coupling is given by

$$I = I_0 \frac{(1-R)^2}{2[(1-R) + kl]} \quad (1)$$

where k is the absorption coefficient, R the reflectivity of the mirrors and l is the cavity length, as derived from the analysis given in [20]. From this expression we can derive that when $kl \ll 1 - R$,

$$\frac{I}{I_0} \approx \frac{1-R}{2} \left(1 - \frac{kl}{1-R}\right). \quad (2)$$

So, for a weak absorber the effective path length is $L = \frac{l}{1-R}$, and the cavity transmission is $(1-R)/2$.

CES has several advantages compared to multi-pass cell spectroscopy. First, the effective path length with commercially available $R > 99.99\%$ mirrors and a 0.5 m-long empty cavity can exceed 1 km, significantly longer than that obtained with a multi-pass cell. The minimum sample volume is defined by the beam diameter and the cavity length. For a 5 mm beam diameter and a 0.5 m-long cavity, it is only 12.5 cm³, compared to 3500 cm³ for the 100 m multi-pass cell used in the above-described experiments. Furthermore, the cost of a set of highly reflective mirrors is less than that of a multi-pass cell and the gas sensor can also be made more compact and lightweight.

In our experiments, the high finesse cavity was formed by two dielectric mirrors having a specified reflectivity of

99.995% at 5.2 μm and a radius of curvature of 6 m. The mirrors were attached to the ends of a stainless steel tube using adjustable vacuum-tight mountings. The tube was 35.5 cm long with an outer diameter of 38 mm. The room temperature detector used in the experiments with the multi-pass cell was replaced by a liquid nitrogen-cooled InSb detector (1 mm² active area) in order to detect weaker signals. The pre-amplified output signal did not exceed several mV, which is within the dynamic range of the detector and the pre-amplifier combination (1 V). As the laser frequency is scanned and the beam is directed along the axis of the optical cavity, high transmission occurs if the laser frequency accidentally coincides with a cavity resonance frequency. For each frequency scan, we observed a number of spikes with a sharp rise and a $\sim 3 \mu\text{s}$ decay, which are caused by the random coincidence of the laser frequency with a cavity resonance (Fig. 4a). A magnitude of each spike was ~ 3 to 4 times higher than the average throughput power. Alignment of the cavity mirrors and the laser beam was made so as to maximize the number of such spikes, which corresponded to a maximum in the number of transversal modes involved. The averaging of many frequency scans resulted in a washout of these spikes, because of the jitter of the resonant frequencies of the unstabilized cavity (Fig. 4b).

2.2 Detection limit and dynamic range

An absorbing gas inside the cavity leads to a decrease in transmitted intensity at a certain frequency and also to a decreased resonator Q-factor. Figure 5 shows an example of two absorption spectra after the averaging of 10 000 scans. These absorptions result from water, CO₂, and NO in a sample of ambient air at 30 Torr (solid line) and breath at 30 Torr (dashed line), which was exhaled through the nose, again by a healthy human subject. For the CES experiments, another NO transition, namely the R13.5 with unresolved components at 1920.707 and 1920.716 cm⁻¹ was used, even though the laser power is approximately three times lower at this frequency. The reason for this frequency change was the presence of strong interfering water absorption lines near 1918 cm⁻¹, which would strongly deteriorate the CES sensitivity.

To extract the actual per-length absorption from the data, it is necessary to determine the effective empty-cavity path

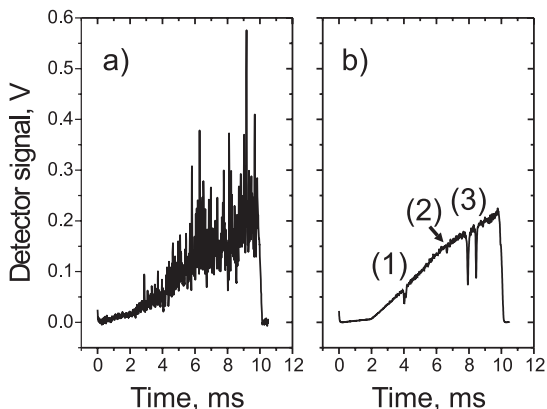


Fig. 4a,b. Transmitted intensity of the CES set-up filled with ambient air at 50 Torr for a single scan (a) and 1000 averaged scans (b). Absorption lines: (1) H₂O at $\sim 1920.9 \text{ cm}^{-1}$; (2) CO₂ at 1920.1 cm^{-1} ; (3) H₂O at 1919.7 cm^{-1} and 1919.5 cm^{-1}

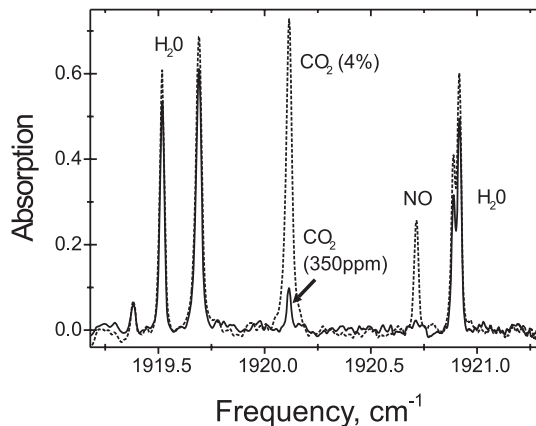


Fig. 5. Absorption spectra of ambient air (solid line) and nasal breath (dashed line) measured using the CES-method at a pressure of 30 Torr

length in a given geometrical configuration. For this purpose, calibration experiments were performed using a N₂-CO₂ mixture with a known CO₂ concentration (Fig. 6). The measured relative transmission of the cavity at the center of the CO₂ absorption line was fitted with the function (3)

$$\frac{I_i - I_t}{I_t} = \frac{kl}{(1 - R_{\text{eff}}) + kl} \quad (3)$$

where I_i is the incident light intensity and I_t is the transmitted intensity. From the data, it was calculated that $R_{\text{eff}} = 0.99942$ and $L = 670 \text{ m}$. The discrepancy between R_{eff} and the manufacturer-specified R value is partially due to the required use of a large number of higher-order transverse cavity modes, which have higher diffraction losses. The absorption was increased by a factor of 6.7 in comparison to the multi-pass cell. However, the minimum detectable absorption was found to be only 1%, which is two orders of magnitude poorer than that found with the optical multi-pass cell technique described in Sect. 1.1. The reason for the high noise in the transmitted intensity is incomplete averaging of the occasional resonance spikes, as well as different losses for different transversal cavity modes. Even with piezo modulation of the position of one cavity mirror and a small modulation in

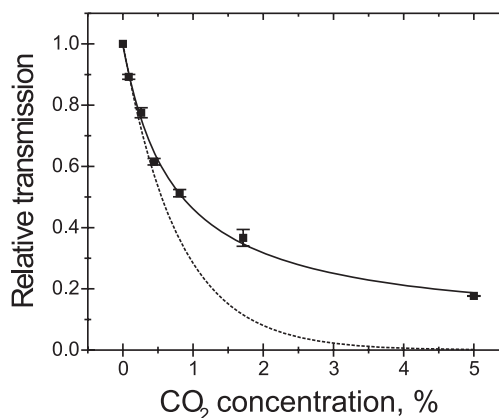


Fig. 6. Relative transmission of the CES-cavity for different CO₂ concentrations from 0% to 5% and a hyperbolic curve fit (solid line) from (3). The dotted line shows the calculated transmission for a multi-pass cell with the same path length as the CES-cell for low CO₂ concentrations

the laser frequency, as proposed in [20], it was not possible to reduce the baseline fluctuations below this limit. This result is in agreement with the data in [20], which correspond to the minimum detectable absorption of $\sim 2\%$.

The NO concentration in the breath sample was evaluated to be 70 ppb with a detection limit ~ 16 ppb, based on a SNR of 1, knowing R_{eff} and the absorption coefficient of the NO R13.5 transition (from the HITRAN'92 database). The CES technique is probably inapplicable for measuring NO concentrations below ~ 10 ppb (as in air exhaled from mouth), but can be used for some other biomedical applications. For example, a typical NO concentration in air exhaled through nose is much higher (~ 100 ppb) and can be successfully measured with CES.

Figure 6 illustrates another feature of CES, which utilizes the selective enhancement of weaker absorption lines. While the weak lines ($kl \ll 1 - R$) are enhanced $1/(1 - R)$ times, as derived from (3), the stronger lines saturate more slowly than with an exponential law, as would be the case for the optical multi-pass cell with an equivalent optical path length. In Fig. 6, the dotted line shows the transmitted intensity expected for a multi-pass cell with the same path length as the effective low-absorption CES path length (670 m). The CES cavity has a transmission of 20% (compared to the evacuated cavity), whereas the transmission of the multi-pass cell becomes only 1.8×10^{-3} , resulting in a signal strength which may be too low to be measured. This characteristic feature enables simultaneous measurement of lines that strongly differ in strength, as is often the case in isotopic composition measurements.

3 Future development

The multi-pass cell-based gas sensor can be made more compact and maintenance-free by replacing a cw liquid nitrogen-cooled laser with a near-room temperature operating pulsed QC-DFB laser. Such devices are already available. It was demonstrated in [21] that a pulsed laser-based detector with an optical multi-pass cell can provide essentially the same level of sensitivity as a cw system. However, the more compact CES configuration requires a cw QC-DFB laser. Although such devices can presently operate only at cryogenic temperatures, there is a strong hope that in the future thermoelectrically-cooled cw operation will be possible. To suppress the cavity-related noise in cavity-enhanced spectroscopy, it is necessary to excite only one transverse mode and directly measure the ring-down time, similar to [22]. This approach should enable a sensitivity of several ppb or better to be reached, as required by biomedical applications.

4 Conclusions

The two experiments showed that it is possible to detect gases such as NO, CO₂ and H₂O vapor simultaneously in exhaled

breath using QC-DFB laser-based IR absorption spectroscopy at 5.2 μm with a frequency scan of 0.5 cm^{-1} (~ 15 GHz). The detection limit for NO was estimated to be 3 ppb when a 100 m path length multi-pass cell was used, and 16 ppb with a CES technique. The integration time was 200 s for optimum sensitivity. For time-integrated concentration measurements (as in nitrite and nitrate concentration measurements in liquid samples, by converting these ions into NO), both techniques should perform comparably to the chemiluminescence technique.

Acknowledgements. The authors acknowledge useful discussions with Prof. Ferid Murad and Dr. Mohammed Bhuiyan from the Department of Integrative Biology and Pharmacology of the University of Texas-Medical School. Financial support of the work performed by the Rice group was provided by the National Aeronautics and Space Administration, the Institute for Space Systems Operations, the Texas Advanced Technology Program, the National Science Foundation, and the Welch Foundation. The Bell Laboratories team received partial support from the Defense Advanced Research Projects Agency/US Army Research Office under Grant No. DAA G 55-98-C-0050.

References

1. F. Muñoz-López: *Allergol. Immunopathol.* **28**, 43 (2000)
2. M. Phillips: *Sci. Am.* **276**, 74 (1992)
3. C. Shimamoto, I. Hirata, K. Katsu: *Hepato-Gastroenterology* **47**, 443 (2000)
4. J.C. de Jongste, K. Alving: *Am. J. Respir. Crit. Care Med.* **162**, 23 (2000)
5. M. Peeters: *Acta Gastroenterol. Belg.* **61**, 332 (1998)
6. E. Culotta, D.E. Koshland: *Science* **258**, 1862 (1992)
7. K. Alving, E. Weitzberg, J.M. Lundberg: *Eur. Respir. J.* **6**, 1368 (1993)
8. N. Wilson, S. Pedersen: *Am. J. Respir. Crit. Care Med.* **162**, 48 (2000)
9. S.J. Chung, H.L. Fung: *Anal. Lett.* **25**, 2021 (1992)
10. A. Fried, S. Sewell, B. Henry, B.P. Wert, T. Gilpin, J.R. Drummond: *J. Geophys. Res.* **102**, 6253 (1997)
11. A.A. Kosterev, R.F. Curl, F.K. Tittel, C. Gmachl, F. Capasso, D.L. Sivco, J.N. Baillargeon, A.L. Hutchinson, A.Y. Cho: *Appl. Opt.* **39**, 4425 (2000)
12. S.W. Sharpe, J.F. Kelly, J.S. Hartman, C. Gmachl, F. Capasso, D.L. Sivco, J.N. Baillargeon, A.Y. Cho: *Opt. Lett.* **23**, 1396 (1998)
13. D.D. Nelson, M.S. Zahniser, J.B. McManus, J.H. Shorter, J.C. Wormhoudt, C.E. Kolb: *Proc. SPIE* **2834**, 148 (1996)
14. P. Mürztz, L. Menzel, W. Bloch, A. Hess, O. Michel, W. Urban: *J. Appl. Physiol.* **86**, 1075 (1999)
15. M. Koch, X. Luo, P. Mürztz, W. Urban, K. Mörke: *Appl. Phys. B* **64**, 683 (1997)
16. F. Capasso, C. Gmachl, D.L. Sivco, A.Y. Cho: *Phys. World* **12**, 27 (1999)
17. Private communications with J.N. Baillargeon, C. Gmachl
18. R. Engeln, G. Berden, R. Peeters, G. Meijer: *Rev. Sci. Instrum.* **69**, 3763 (1998)
19. R. Peeters, G. Berden, A. Apituley, J. Meijer: *Appl. Phys. B* **71**, 231 (2000)
20. A. O'Keefe, J.J. Scherer, J.B. Paul: *Chem. Phys. Lett.* **307**, 343 (1999)
21. A.A. Kosterev, F.K. Tittel, C. Gmachl, F. Capasso, D.L. Sivco, J.N. Baillargeon, A.L. Hutchinson, A.Y. Cho: *Appl. Opt.* **39**, 6866 (2000)
22. B.A. Paldus, C.C. Harb, T.G. Spence, R.N. Zare, C. Gmachl, F. Capasso, D.L. Sivco, J.N. Baillargeon, A.L. Hutchinson, A.Y. Cho: *Opt. Lett.* **25**, 666 (2000)